Study on the characteristics of compressive strength and hydration mechanism of high-water-content materials modified by furnace slag and silica fume

Study on the characteristics of compressive strength and hydration mechanism of high-water-content materials modified by furnace slag and silica fume

Lianwei Zhang[1,2], Changwu Liu[1,2*], Fan Wu[3], Yonghu Lu[1,2], Xianliang Zhou[1,2]

[1]State Key Laboratory of Hydraulics and Mountain River Engineering, Sichuan University, Chengdu, Sichuan, 610065, China

[2] College of Hydraulic Engineering, Sichuan University, Chengdu, Sichuan, 610065, China

[3] Institute of Disaster Management and Reconstruction, Sichuan University- The Hong Kong Polytechnic University, Chengdu, Sichuan, 610065, China

[*]Corresponding author's e-mail: liuchangwu@scu.edu.cn

Abstract. In order to reduce the economic cost of high-water-content materials used in mine filling and improve the resource utilization rate of furnace slag and silica fume, furnace slag and silica fume were mixed into high-water-content materials by the admixture method. The variation law of compressive strength, hydration mechanism and microstructure were analyzed. When the furnace slag content is 10%, the compressive strength of high-water-content materials modified with furnace slag is consistent with that of pure high-water-content materials. When the silica fume content is 10% and 20% respectively, the compressive strength of high-water-content materials modified with silica fume increases by 8.54% and 3.66% respectively compared with pure high-water-content materials. When the furnace slag content is 30%, SiO_2 in slag snatches Ca^{2+} and OH^- from the solution to form a large amount of c-s-h gel, and the insufficient Ca^{2+} greatly hinders the formation of AFt crystals. When the silica fume content is 40%, the diffraction peak of AFt crystals cannot be observed in the diffraction pattern, which further indicates that the content of AFt crystals is an important factor affecting the compressive strength of high-water-content materials. When the content of slag and silica fume is low, AFt crystals are mostly in fine needle shape, the overall structure is uniform and dense. When the content of furnace slag and silica fume is high, AFt crystals are mostly of coarse columnar shape, and the overlapping mode becomes sparse and chaotic, and the dense degree of structure is seriously reduced.

1. Introduction

High-water-content materials are a major breakthrough of concrete materials, which not only have various properties compared with ordinary concrete, but also have the characteristics such as high water content and quick setting that ordinary concrete does not have. High-water-content materials can be mixed with nine times the volume of water to form a hardened body with a certain strength in 30 min[1]. Due to the advantages of high-water content, high strength in the early stage, fast coagulation speed and simple manufacturing process, high-water-content materials have been widely used in roadway support and goaf filling of mining engineering and leaking stoppage and foundation reinforcement of underground engineering. And the application of high-water-content materials has

solved the long-standing problem of gob-side entry retaining in the coal mine, prolonged the service life of the mine and improved the safety of the work surface[2]. The research and development of high-water-content materials are a major technological breakthrough in mining engineering and have good social and economic benefits.

However, there are still some problems in the actual engineering application of high-water-content materials. For example, high-water-content materials often have some problems during mixing such as water bleeding, stratification and segregation[2]; With the high water-cement ratio, the filling cost of high-water-content materials decreases, but the compressive strength also decreases[3]; The over rapid hydration reaction speed and condensation speed of high-water-content materials results in high strength in early stage and insufficient strength in later stage[4]. In recent years, a large number of scholars at home and abroad have carried out doping modification of high-water-content materials in an attempt to improve a series of defective conditions in high-water-content materials. Chen Hongling mixed clay minerals into high-water-content materials, and the results showed that mixing proper amount of clay minerals could improve the uniformity of slurry and reduced the water bleeding[2]; In the compressive strength test, Wu Meisu found that when the slag powder content was 20%, the uniaxial compressive strength of the slag modified high-water-content materials was higher than that of pure high-water-content materials, which had increased by 13.33%[3].

Furnace slag is an industrial solid waste generated by coal burning in the process of thermal power generation. At present, the annual discharge of furnace slag in China has exceeded 500 million tons. The furnace slag utilization rate is very low under such high discharge amount, and is commonly used for paving brick. The application of admixture is far less than that of fly ash. How to rationalize and utilize it, not only relates to environmental benefits but also to economic benefits and technical benefits[5-6]. Silica fume is industrial dust collected in flue gas purification equipment during high temperature silicon refining and ferrosilicon alloy. China produces about 250,000 tons of silica ash per year. Currently, silica fume is mainly used as concrete admixture to improve its working performance. The development of silica fume is huge, and how to further deepen its research has become a hot topic[7].

In this paper, furnace slag and silica fume were mixed into high-water-content materials to explore the effect of furnace slag and silica fume on the compressive strength of high-water-content materials, and the hydration mechanism analysis and microstructure analysis of furnace slag and silica fume modified high-water-content materials were carried out.

2. Experimental design

2.1. Experimental materials

The high-water-content materials contain four kinds of ingredients. Among them, the minerals of the material A mainly include $3CaO·3Al_2O_3·CaSO_4$（$C_4A_3\overline{S}$） and $2CaO·SiO_2$（C_2S）, and the minerals of the material B mainly include $CaSO_4·2H_2O$ and CaO; The material A-A and the material B-B are a retarder and a quick setting agent, respectively. The furnace slag used in the test originates from a thermal power plant in Huainan, Anhui Province. The furnace slag was ground in a mortar, and X-ray diffraction analysis was performed after sample preparation. As shown in Figure 1, The diffraction peaks of crystalline minerals such as $3Al_2O_3·2SiO_2$, SiO_2, $CaSO_4·2H_2O$, $CaCO_3$ and $Ca(OH)_2$ are strong; the silica fume used in the experiment originates from a special silica fume production plant in Sichuan, and the purity of silica fume is high, and the content of SiO_2 is above 95%.

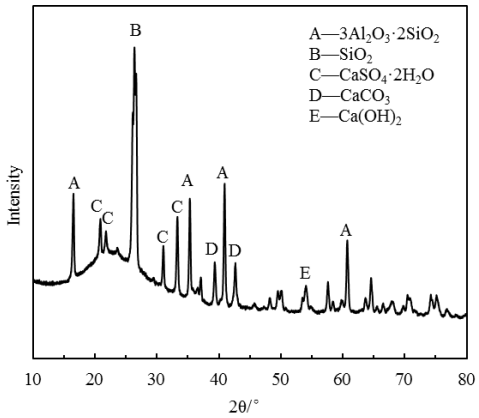

Figure 1. XRD patterns of fine-grained furnace slag

2.2. Experimental plan

The water-cement ratio of the high-water-content materials is set to 4:1, at the same time, the pure high-water-content materials are set as control group; The furnace slag modified high-water-content materials are represented by LGS; the silica fume modified high-water-content materials are represented by GGS; the furnace slag and silica fume double mixed into materials are represented by GLGS; the pure high-water-content materials are represented by CGS. The proportion of CGS, LGS, GGS and GLGS is shown in Table 1.

Table 1. Ratio of high-water-content materials

Group	Serial number	Amount of admixture/%	A /g	A-A /g	B /g	B-B /g	Slag /g	Silica fume /g
CGS	C	—	180	18	180	7.2	—	—
LGS	L10	10	180	18	180	7.2	18	—
	L20	20	180	18	180	7.2	36	—
	L30	30	180	18	180	7.2	54	—
	L40	40	180	18	180	7.2	72	—
GGS	G10	10	180	18	180	7.2	—	18
	G20	20	180	18	180	7.2	—	36
	G30	30	180	18	180	7.2	—	54
	G40	40	180	18	180	7.2	—	72
GLGS	G10L10	20	180	18	180	7.2	18	18
	G10L20	30	180	18	180	7.2	36	18
	G10L30	40	180	18	180	7.2	54	18

2.3. Preparation and maintenance of samples

According to the proportion in Table 1, the high-water-content materials specimens were prepared, and the A material and the A-A material were mixed with water to prepare Slurry-I, and the B material and the B-B material were mixed with the remaining water to prepare Slurry-II, and Slurry-I and Slurry-II were mixed and stirred around the basin wall. After the slurry was evenly stirred, it was poured into a cylindrical mold with an inner diameter of 50 mm (height: inner diameter = 2:1). After one day of constant temperature curing, the surface was smoothed, and then the specimens after removal from mould were maintained in the water tank at 20 ℃. After 7 days of curing, the specimens were taken out for experiment.

3. Compressive strength test results

3.1. Stress-strain curve

Taking C, L20, G30 and G10L20 as examples, the stress-strain curves of CGS, LGS, GGS and GLGS

during the compression process are shown in Figure 2.

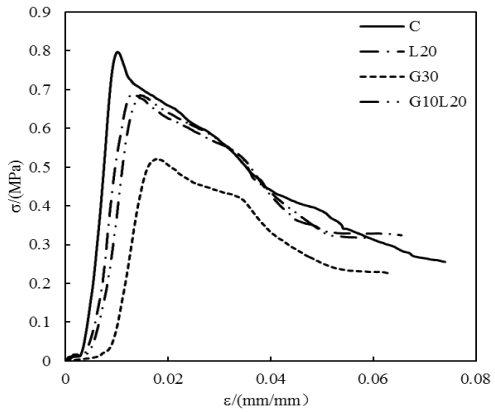

Figure 2. Stress-strain curve of high-water-content materials

It can be seen from Figure 2 that at the stage when the axial load is just applied, the micropores, micro-cracks and unclosed pores inside the specimens are gradually compacted; as the load increases, the specimens elastically deforms, the stress increases sharply, and the strain increases slowly. At this stage, there is water droplet concentration at the bottom of the specimens. When the axial load continues to increase, visible micro-cracks on the surface of the specimens begin to appear, and the more concentrated the stress is, the more obvious the micro-crack is; when the specimens reach the failure stage, the specimens fracture occur under the stress of the axial load. The surface of the fracture continues to bear the load and exhibits good residual load carrying capacity. The specimen below the fracture surface provides support for the specimen above the fracture surface, which keeps the specimen to maintain integrity although it is damaged. It is further indicated that the high-water-content materials belong to the filling materials with elastoplastic deformation characteristics, which are different from the rock materials as they still have a strong retention ability when the body is cracked or even damaged.

3.2. Effect of single-mixed furnace slag and silica fume on compressive strength of high-water-content materials

As shown in Figure 3, when the furnace slag content is 10%, the compressive strength of LGS and CGS is 0.82 MPa, respectively; when the furnace slag content is in the range of 10~30%, the compressive strength decreases stepwise, and the decrease is obvious; the compressive strength of LGS appears at a minimum at 40% furnace slag content, which is 63.41% of CGS. When the content of silica fume is 10% and 20% respectively, the compressive strength of GGS is 8.54% and 3.66% higher than that of CGS. When the content of silica fume is between 20% and 40%, the compressive strength decreases stepwise, and the decrease is large; the compressive strength of GGS shows a minimum at 40% silica fume content, which is 63.63% of CGS.

When the additive content of the added material is less than 40%, and under the same mixed dosage, the compressive strength of GGS is always higher than that of LGS, and the increase of compressive strength ranges from 1.92 to 19.64%. When the additive content is 20%, the increase reaches the maximum value.

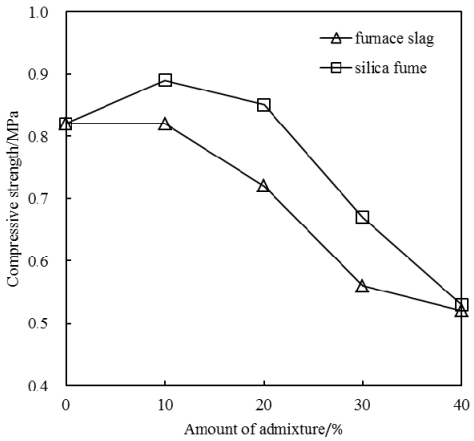

Figure 3. Compressive strength of high-water-content materials with different content of furnace slag and silica fume

3.3. Effect of double-mixed furnace slag and silica fume on compressive strength of high-water-content materials

Figure 4 shows the compressive strength of LGS, GGS and GLGS under different doping conditions. When the additive content is 20%, the compressive strength of GGS is greater than LGS and GLGS; when the added substance content is 30% and 40%, respectively, the compressive strength of GLGS is greater than that of LGS and GGS. More obviously, when the additive content is 40%, the compressive strength of GLGS is 50% and 47.17% higher than that of LGS and GGS, respectively. It shows that under the condition of small additive content, the compressive strength of the silica fume modified high-water-content materials can achieve the most ideal effect; under the condition of large additive content, the materials double mixed with furnace slag and silica fume can achieve the most ideal effect.

Further analysis shows that the compressive strength and the mixed content of LGS and GGS are negatively correlated. Under the double-mixed condition, the compressive strength of GLGS shows an overall increasing trend, which further indicates that the double-mixed method is more reasonable to be adopted under the condition of large dosage.

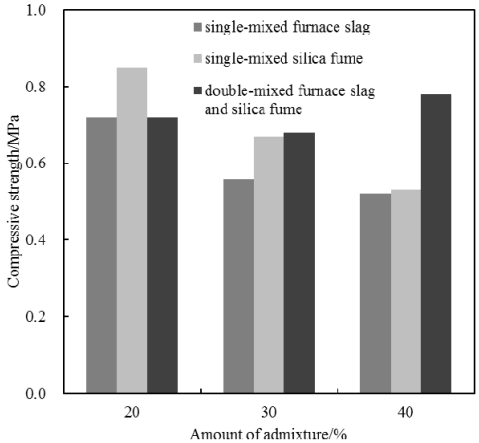

Figure 4. Compressive strength of high-water-content materials under different doping conditions

4. Hydration mechanism analysis and microstructure analysis

4.1. Analysis of hydration mechanism

The hydration products of CGS mainly include AFt crystals ($3CaO{\cdot}Al_2O_3{\cdot}3CaSO_4{\cdot}32\ H_2O$), C-S-H

gel, aluminum gel ($Al(OH)_3$) and $Ca(OH)_2$. The hydration reaction of CGS is shown as equation (1), (2) and (3)[1], when the content of $CaSO_4$ is small, part of $C_4A_3\overline{S}$ reacts according to equation (1) to form AFt crystals, and form a dense and hard skeleton in a short time; C_2S reacts to produce C-S-H gel by equation (2). When the content of $CaSO_4$ remains, the $Ca(OH)_2$ precipitated in the equation (2) is further consumed according to the formula (3) to form AFt crystals.

$$3CaO\cdot3Al_2O_3\cdot CaSO_4+2CaSO_4+38H_2O\rightarrow3CaO\cdot Al_2O_3\cdot3CaSO_4\cdot32\ H_2O+4Al(OH)_3 \quad (1)$$

$$2CaO\cdot SiO_2+(2\text{-}m+n)H_2O\rightarrow mCaO\cdot SiO_2\cdot nH_2O+(2\text{-}m)Ca(OH)_2 \quad (2)$$

$$3Ca(OH)_2+3CaSO_4+2Al(OH)_3+26H_2O\rightarrow3CaO\cdot Al_2O_3\cdot3CaSO_4\cdot32H_2O \quad (3)$$

As shown in Figure 5, the hydration products of LGS include AFt crystals, SiO_2, C-S-H gel, $3Al_2O_3\cdot2SiO_2$, $Al(OH)_3$, and $CaCO_3$. The diffraction peaks of $Ca(OH)_2$ and C-A-H cannot be found in the spectrum. This is because $Ca(OH)_2$, which forms by the hydration of $CaO\cdot SiO_2$, participates in the secondary hydration reaction. $Ca(OH)_2$ is generated, and it is consumed later, so it cannot be detected. Because the content of Al_2O_3 in the furnace slag is small, only little C-A-H is generated in the slurry, and the XRD instrument itself is not accurate enough, so the diffraction peak of C-A-H is not obvious enough to be detected. Under different slag mixing amount, the hydration products of LGS are basically the same, but the diffraction peaks intensity of hydration products are different. Although the diffraction peak intensity does not represent the true percentage of each phase, the diffraction peak intensity of each phase is indeed related in a certain degree with the content of each phase. With the increase of furnace slag content, the diffraction peaks intensity of AFt crystals, $3Al_2O_3\cdot2SiO_2$ and C-S-H gel are weakened, enhanced and enhanced, respectively, which indicates that the production of AFt crystals, $3Al_2O_3\cdot2SiO_2$ and CSH gel decreases, increases and increases respectively as the mixing amount of furnace slag increases.

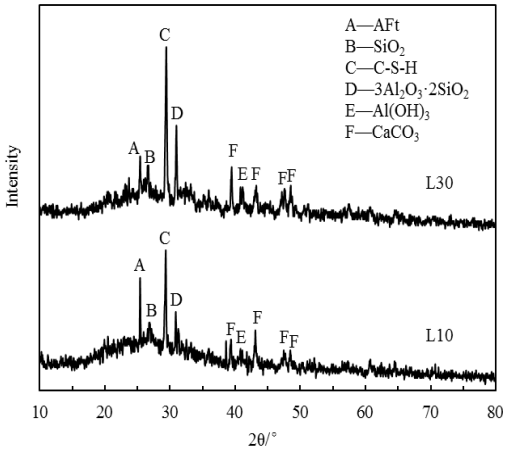

Figure 5. XRD patterns of high-water-content materials with furnace slag

After being mixed with the furnace slag, SiO_2 and Al_2O_3 in the slag react with $Ca(OH)_2$ according to formula (5) and (6) to form C-S-H and C-A-H[8-10]. When the content of slag is small, $Ca(OH)_2$ formed by the formula (2) is sufficient to provide $Ca(OH)_2$ required for the formula (5) and (6), therefore, the number of AFt crystals generated by the formula (3) will not being affected. The compressive strength of LGS can be basically the same as CGS; when the slag content reaches 30%, the $Ca(OH)_2$ required by formula (5) and (6) does not have sufficient supply of formula (2). Remaining SiO_2 and Al_2O_3 capture the $Ca(OH)_2$ formed by formula (2) at a faster reaction rate, and formula (3) is greatly affected, resulting in a decrease in the number of AFt crystals and an increase in the amount of C-S-H gel. With the gradual increase of slag content, SiO_2 and Al_2O_3 gradually react to form $3Al_2O_3\bullet2SiO_2$ under alkaline slurry conditions, which directly leads to a decrease in the compressive strength of LGS under high slag mixed content conditions since the AFt crystals are important products that affect the compressive strength characteristics of high-water-content materials.

$$CaO+H_2O\rightarrow Ca(OH)_2 \quad (4)$$

$$SiO_2+m_1Ca(OH)_2+n_1H_2O\rightarrow m_1CaO\cdot SiO_2\cdot(m_1+n_1)\ H_2O \quad (5)$$

$$Al_2O_3+m_2Ca(OH)_2+n_2H_2O\rightarrow m_2CaO\cdot Al_2O_3\cdot(m_2+n_2)H_2O \quad (6)$$

As shown in Figure 6, it can be found that when the content of silica fume is 10%, the hydration products are AFt crystals, SiO_2, C-S-H gel, $3Al2O_3\cdot 2SiO_2$, $Al(OH)_3$ and $CaCO_3$; when the content of silica fume is 40%, the hydration products only have C-S-H gel, $3Al_2O_3\cdot 2SiO_2$, $Al(OH)_3$ and $CaCO_3$. The diffraction peak of AFt crystals is not found in the spectrum. The diffraction peak of C-S-H gel is generally unchanged, and its diffraction peak reaches the highest in the spectrum. The diffraction peak of $3Al_2O_3\cdot 2SiO_2$ is slightly enhanced, which indicates that the formation of AFt crystals is significantly affected by the high silica fume content, and the content of $3Al_2O_3\cdot 2SiO_2$ is slightly increased.

The reason is that $Ca(OH)_2$ generated by formula (2) acts as an alkaline activator on silica fume, causing $Ca(OH)_2$ to be absorbed in a large amount, and the concentration of $Ca(OH)_2$ is lower, which accelerates the hydration speed of $2CaO\cdot SiO_2$ and silica fume, C-S-H gel and aluminum gel fill the unclosed pores in the samples at the same time, thus increasing the compressive strength of GGS, but the amount of silica fume should not be too large, otherwise the AFt crystals generation will be extremely affected. Zhang Lijun and Wang Lei [11-12] believe that the dispersion of silica fume plays a role of crystals nucleation when mixing mortar. On the one hand, it reduces the concentration of alkali in the mortar, on the other hand, it makes the hydration products (CSH gel and aluminum gel) uniformly distributed in the mortar, but the amount of silica fume should be controlled within a certain range, otherwise the dispersion of excess silica fume will directly reduce the compressive strength of the materials.

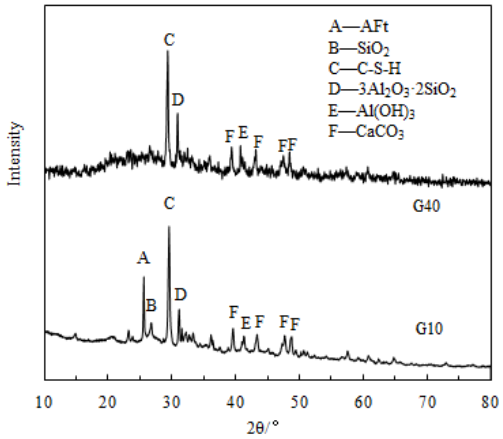

Figure 6. XRD patterns of high-water-content materials with silica fume

$$SiO_2+ xCa(OH)_2+H_2O\rightarrow xCaO\cdot SiO_2\cdot(x+1)H_2O \quad (7)$$

4.2. Microstructure analysis

Taking L10, L30, G10 and G40 as examples, the microstructures of LGS and GGS are shown in Figure 7. During the coagulation process, the materials rapidly hydrate to form a large number of AFt crystals, C-S-H gel, $3Al_2O_3\cdot 2SiO_2$, $Al(OH)_3$ and $Ca(OH)_2$, and the AFt crystals are intertwined and overlaps each other to form a branched network structure. The C-S-H gel has a fibrous structure, and the crystals of $3Al_2O_3\cdot 2SiO_2$ are elongated and acicular, and $Al(OH)_3$ has a misty sheet structure. At this stage, many strong and weak contact points are generated between the products. The contact points connect the fine particles inside the high-water-content materials into a net. As the hydration reaction continues, the contact points increase continuously, and the branch network structure is more disorderly intertwined, making the high-water-content materials skeleton structure more perfect and compressive and the intensity increases accordingly.

In the small dosage range, the AFt crystals are formed at a high speed in an alkali with solution high concentration, and are mostly in the shape of fine needles, and the overlap between the AFt crystals is compact, the overall structure is relatively uniform and compact, and has a high load

carrying capacity; In the range of large dosage, the formation of AFt crystals in lower alkali solution is slower, mostly in the form of coarse column, and the uniformity of the branched network structure is reduced. The bonding between AFt crystals becomes sparse and chaotic, and a large number of pores are obviously observed, and the densification of the dendritic structure is severely reduced, resulting in a decrease in the compressive strength of LGS and GGS under high mixed content conditions[13].

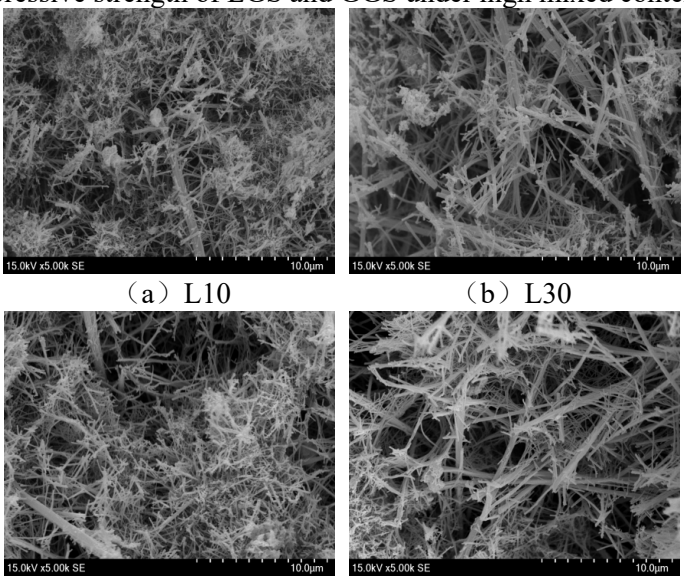

（a）L10 （b）L30

（c）G10 （d）G40

Figure 7. The microstructure of high-water-content materials

Figure 8 shows the microstructure of G10L30, the magnification is 3000 times and 8000 times, respectively. It can be seen from Figure 8 that the high-water-content materials exhibit a different microstructure under the double doping condition compared with the single doping condition, The dendritic structure of AFt crystals becomes inconspicuous, and the fibrous hydrated calcium silicate gel, the misty aluminum paste and the incompletely reacted slag residue fill the pores of the dendritic structure, so that the overall structure becomes abnormally dense, and high-water-content materials still have high compressive strength under high dosage conditions.

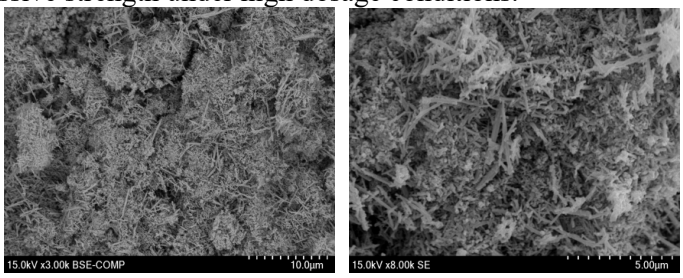

（a）3000 times （b）8000 times

Figure 8. The microstructure of G10L30

5. Conclusion

1) When the furnace slag content is 10%, the compressive strength of the furnace slag modified high-water-content materials is consistent with the compressive strength of the pure high-water materials; when the silica fume content reaches 10% and 20%, compared with pure high-water-content materials, the compressive strength of the silica fume modified high-water-content materials increases by 8.54% and 3.66%, respectively.

2) When the mixed dosage is small, the compressive strength of silica fume modified high-water-content materials can achieve the most ideal effect; Under the condition of large mixed dosage, the furnace slag and silica fume modified high-water-content materials can achieve the most

ideal effect, which indicates that furnace slag and silica fume can be incorporated into high-water-content materials. Appropriate amount of slag and silica fume can play a role in improving the compressive strength of high-water-content materials.

3) The hydration products of LGS include AFt crystals, SiO_2, C-S-H gel, $3Al_2O_3•2SiO_2$, $Al(OH)_3$ and $CaCO_3$. When the furnace slag content is increased to a higher level, SiO_2 captures $Ca(OH)_2$ formed by hydration of $2CaO·SiO_2$ to react in a faster reaction rate, resulting in a decrease in the formation of AFt crystals. The excess SiO_2 and Al_2O_3 gradually react to produce $3Al_2O_3•2SiO_2$ in the alkaline slurry condition.

4) When the dosage is in the lower range, the AFt crystals are formed faster in the high concentration alkali solution, and it is mostly in the shape of fine needles. The overall structure is more uniform and denser. When the dosage is in the higher range, the AFt crystals formation rate is slow in the low concentration of alkali solution, which mostly in the shape of a thick column, and the overlapping structure between the AFt crystals becomes sparse and chaotic.

References

[1] Sun H., Song C. (1994) High water quick setting material and its application. Jiangsu Xuzhou: China University of Mining and Technology Press.
[2] Chen H., Wang Y. (2010) Modification of clay material for high-water material based on sulphoaluminate cement. Building Science Research of Sichuan., 36(2) :240-243.
[3] Wu M., Liu C. (2018) Study on physical and mechanical properties of modified high-water material with different content of slag powder. Metal Mine., (1): 63-67.
[4] Feng B., Liu C., Xie H., et al. (2018) Experimental study and mechanism analysis of mechanical properties of fly ash modified high water material. Engineering Science,. 40(10): 1187-1195.
[5] Pan P., Ou Yang D., Yi C., et al. (2011) Effects of coal bottom ash on properties of high-performance Concrete . China Concrete and Cement Products, . (6): 19-22.
[6] Zhang L., Li J., Liu F. (2017) Influence of activating cinders power to recycled concrete performance . Concrete,.(5): 72-74.
[7] Wu M., Liu C., Jiang Y, et al. (2017) Experimental study on the influence of typical suspension additives on mechanical properties of high-water materials. Advanced Engineering Sciences, . 49(S1) : 21-26.
[8] Hu H.,Ma B., et al. (2016) Concrete mineral admixture. Beijing: China electric power press.
[9] Zhang Y., Liu C., Xie H., et al. (2017) Experimental research on the effects of water-cement ratio on mechanical properties of high-water materials. Journal of Sichuan University (Engineering Science Edition),. 49(S2): 115-120+127.
[10] Zhang G., Zhong Z., et al. (2016) Building materials. Beijing: China electric power press.
[11] Zhang L. (2004) Study on the early electrical behavior and hydration activity of different mineral admixtures. Wuhan University, Wuhan.
[12] Wang L., He Z., Yang H., et al. (2013) The microcosmic mechanism of silica powder to enhance the abrasion resistance of concrete. Hydraulic Engineering,. 44(1):111-118.
[13] Xie H., Liu C. (2014) Analysis on raw material of high-water and quick-setting material stone. Science Technology and Engineering,. 14(30):254-257+271.